Model of Combustion Synthesis of Thermoelectric Calcium Cobaltates

Jiri Selig and Sidney Lin*
Dan F. Smith Department of Chemical Engineering, Lamar University, Beaumont, Texas, USA
*Corresponding author: Lamar University, P.O. Box 10053, Beaumont, TX 77710, USA
sidney.lin@lamar.edu

Abstract: Thermoelectric materials generate an electrical potential from a temperature difference and are widely used to convert waste heat into usable electrical power. Thermoelectric oxides, such as calcium cobaltates, are suitable for automobile waste heat recovery because they are stable when contacting high temperature exhaust (~600 ºC). Self-propagating High-temperature Synthesis (SHS), a very economical process to synthesize complex oxides was successfully used in our lab to produce such oxide materials. A mathematical model is needed to study and optimize the synthesis conditions. In this work, a two-dimensional model of SHS of calcium cobaltates using the COMSOL Multiphysics package was generated. Momentum, heat, and mass transfers as well as reaction kinetics are included and coupled in the model. The model shows detailed reaction front movement and a narrow reaction zone. Calculated results including the reaction rate and temperature profile are compared to experimental data to confirm its validity.

Keywords: Thermoelectric, Ceramics, Finite Element Analysis

1. Introduction

Twenty one peta-Btu ($21x10^{15}$ Btu) of waste heat is released to environment from automobile exhaust which has a temperature above 600 °C via automobile tail pipes in the US in 2008.[1] This heat loss not only reduces the fuel efficiency but also produces heat pollution impacting the climate change. Recovering this waste is the solution to both problems. A simple estimate shows the electrical power generated by recovering 1% of the automobile waste heat is sufficient to power all electrical/electronic devices except the headlight in a car**.**

Thermoelectric devices utilize a temperature difference to generate electrical current. The Seebeck effect describes the generation of an electrical current in a closed loop when there is a temperature difference between two leads.[2] In recent years, the Seebeck effect is used to generate electrical power for electronic equipment in automobiles from their exhaust heat. For example, BMW will launch new vehicles equipped with the thermoelectric power generator in 2014.[3]

Calcium cobaltates (e.g. $Ca_{1.24}Co_{1.62}O_{3.86}$) are good candidates for thermoelectric applications in oxidizing environment.[4] These materials have good thermoelectric properties due to their intricate layered structure that combine electrical conducting CoO_2 layers and insulating Ca_2CoO_3 substructure.[5] This substructure approach helps to separate the electrical and thermal properties of the material. The electronic layer keeps a good electrical conductivity in the material while the layered structure increases phonon scattering and thus decreasing thermal conductivity.[6]

Self-propagating High-temperature Synthesis (SHS) is a very efficient method to prepare calcium cobaltates[7]. It was developed in Russia in the late 1960's[8] and has been used to synthesize many ceramic materials including oxides, nitrides, carbides, and metal hydrides.[9,10]

In SHS reactions, reactants consist of fuels (metal powders), oxidizers, and fillers (metal oxides). The ratio of fuel to filler is adjusted to obtain optimal reaction conditions. In some cases, solid oxidizer is added to increase the reaction rate. Reactants are either used in a loose powder form or pressed into pellets. Inside a pressed pellet reactants have better contact which often helps reaction front propagation, but the pellet's higher density also reduces the gaseous reactant diffusion into the pellet which can affect the reaction stability. To initiate the SHS reaction, reactants are ignited by an external heating source. The SHS reaction is highly exothermic and only a small amount of ignition energy is needed. The heat generated from the reaction is sufficient to sustain the reaction and the reaction front propagates from the ignition point through the rest of the pellet. SHS process is usually conducted at room temperature, which

further allows for low energy requirements of the synthesis.

The generally fast combustion front movement (1-100 mm/sec) and easy to scale-up feature enable SHS a large-scale production in a short period of time. Fast heating rate (on the order of 100s K per second) inside the reactant pellet and the fast cooling following the reaction allows the formation of ceramic powders with very fine grains and metastable compositions. The fast reaction process can prevent the forming of thermodynamically preferred compounds. Because of the high temperature SHS reaction can reach many impurities will evaporate this process is self-purifying.

2. Experimental Background

Calcium cobaltate was made by SHS following the stoichiometric equation below:

$$1.24CaO_2 + 1.62Co \xrightarrow{O_2} Ca_{1.24}Co_{1.62}O_{3.86} \qquad (1)$$

Reactants were mixed and then pressed into a pellet 7/8" in diameter. Pressed pellet was placed in a glass reactor and ignited by a graphite igniter. Once the pellet was ignited, the igniter was turned off and reaction front self-propagated through the pellet converting the reactants into the product at a rate of 0.27 mm/s.

Temperature of the reaction was measured by two thermocouples placed at the centerline of the pellet at a known distance apart. Infrared camera was also used to measure the temperature on the surface of the pellet.

3. Model Description

3.1 Geometry

Model geometry was based on our experimental set-up. A two-dimensional analysis was used to reduce the complexity of the model and the solution time. Two solid domains represent the solid pellet and pellet holder, and a fluid domain represents the oxygen in the reactor. Sketch of the geometry is shown in Figure 1. Due to the large temperature gradient during the SHS reaction very fine triangular mesh was used to model the pellet to improve the model convergence. The maximum element size was set to be 2.5×10^{-4}. The pellet holder and fluid domain were mashed more coarsely.

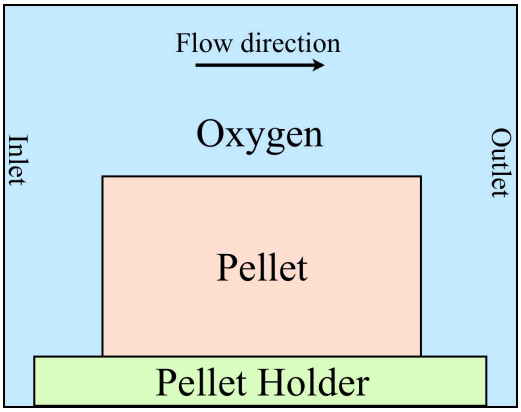

Figure 1. Model geometry (not to scale).

Three different application modes are used in our work. Navier-Stokes equation was used to study the flow of oxygen in the reactor (momentum transfer). Heat balance and mass balance were used to study the gas domain as well as the solid-state domains inside the reaction pellet and pellet holder.

3.2 Momentum balance

Weakly compressible Navier-Stokes equation was used to take into account density variations resulting from the large temperature gradient (room temperature to 1,000 K and above) during the SHS reaction.

The inlet boundary conditions were set to a constant flow rate and the outlet boundary condition was to set to be a constant pressure. All reactor walls and gas/solid interface had no-slip conditions.

3.3 Energy balance

Modified energy balance was used to model the heat-transfer inside the gas and solid domains. The convective term was only used on the fluid domain.

$$\rho C_p \left(\frac{\partial T}{\partial t} + \mathbf{u}\nabla T \right) = \nabla \cdot \left(k\nabla T \right) + Q \qquad (2)$$

Because the pellet is porous the ρC_p term was modified to take into account the porosity of the pellet and its effect on heat transfer.

$$\rho C_p \left(\frac{\partial T}{\partial t} + \mathbf{u}\nabla T \right) = \nabla \cdot (kT) + Q \quad (3)$$

The heat source term, Q, was calculated from the reaction rate and the enthalpy of reaction:

$$Q = \frac{d\eta_r}{dt} \Delta H_r \quad (4)$$

The reaction rate was calculated by the following expression:

$$\frac{d\eta_r}{dt} = (1 - \eta_r)^n k_r \exp\left(\frac{-E}{RT}\right) \quad (5)$$

In this case the reaction order, n, was equal to 1 and value of pre-exponent, k_r, is equal to 500 s^{-1}. Activation energy (E) was calculated from experimental data.

The boundary conditions of the inlet of the reactor and the top reactor wall were set to ambient temperature. The bottom of the reactor was set to be insulation boundary condition and the outlet was set to convective heat flux. The interface between the pellet and oxygen was set to a heat flux to take into consideration the surface heat-loss due to heat convection and heat radiation.

$$-q_0 = h_c(T - T_\infty) + \varepsilon_r \sigma (T^4 - T_\infty^4) \quad (6)$$

The convective heat transfer coefficient was calculated from empirical formula for mixed forced and natural convection[11] and emissivity was set to 0.5.

The pellet was ignited by external heat flux defined by the following expression:

$$q_{ign} = 6\text{x}10^5 \text{ W/m}^2, \text{ (t < 5s)} \quad (7)$$

3.4 Mass balance

Simple mass balance was used to model the conversion of reactants to products. In this work, the diffusion of oxygen into the porous pellet was neglected so the mass balance was simplified to the following equation

$$\frac{\partial c}{\partial t} = R_c \quad (8)$$

Because the reaction order is equal to one in equation 5, the rate expression it can be easily converted to rate expression in terms of concentration and used in equation 8. This can be done by defining conversion as:

$$\eta_r = \frac{c}{c_{\max}} \quad (9)$$

where c_{max} is the maximum product concentration determined from stoichiometric equation and product density.

Since there is no mass transfer between the pellet and oxygen the boundaries were set to be insulation.

4. Results

Temperature profile at 60 s after ignition is shown in Figure 2. This profile is a character of SHS reaction. It shows the large temperature gradient caused by the low thermal conductivity of the sample pellet and the fast reaction rate. There is a visible hot spot near the pellet/oxygen interface which is caused by the low rate of heat loss from the surface of the pellet. The maximum temperature at this instance is 1,326 ºC which agrees with our experimental measurements.

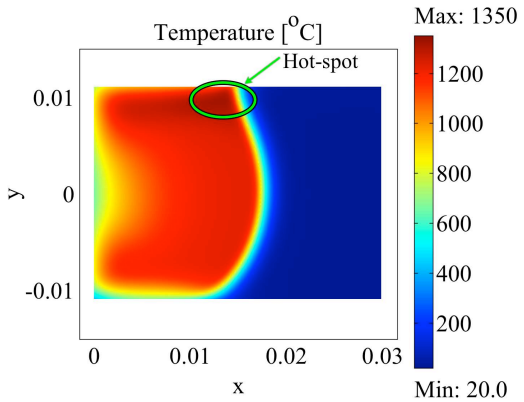

Figure 2. 2D pellet temperature profile at 60s after ignition Reaction propagates from left to right.

Reaction rates inside the pellet are plotted in Figure 3. The figure shows the narrow reaction region of the SHS reaction. Reactants are quickly converted to products (~2 seconds) as the reaction propagates from left to right. Due to the higher temperature near the top surface (as shown in Figure 2) the reaction in the upper region is higher than that in the lower region. Because the heat loss from the pellet to the pellet holder is relatively high, the reaction and temperature are lower in that region.

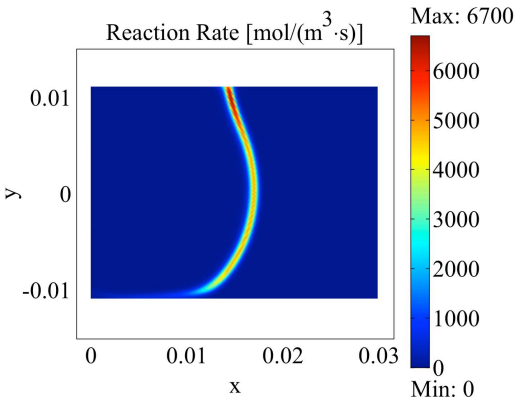

Figure 3. Reaction rate at 60s after ignition. Reaction propagates from left to right.

Results calculated from this model were validated by comparing with our experimental measurements (Figure 4). The temperatures at the centerline of the pellet measured by thermocouples 1.5 cm apart are similar with those at the same two points calculated from our model. The maximum temperature calculated by the model is 50 ºC higher than the measured one. This difference is caused by the lack of a more accurate heat loss from the reacting pellet when the pellet cracks during reaction. The speed of the reaction front movement (the distance between two thermocouples divided by the time difference for these two points to reach the same temperatures) is faster in the model. During our experiments, the reaction front propagated at a speed of 0.27 mm/s. The model predicts a speed of 0.36 mm/s (33% higher). This might be caused by the error in estimating thermal conductivity of the pellet.

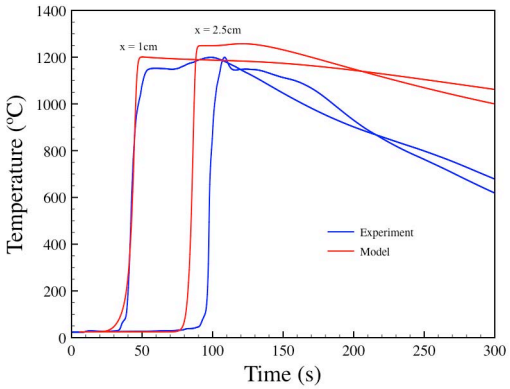

Figure 4. Comparison of experimental results with model prediction.

The measured pellet cooling rate after the reaction is faster due to the cracking of pellet which increases the amount of heat loss. Also, because of the pellet expansion during reaction thermocouples may not be in contacts with the pellet and measure the oxygen temperature instead .

Thermal conductivities of the pellet (reactants and product) were varied by 20% to study its effect on reaction front propagation speed. Increase of thermal conductivity has negligible effect on the temperature at the centerline of the pellet. However, the reaction front propagation speed was noticeably affected. When thermal conductivity is increased the propagation velocity increased from 0.36 mm/s to 0.40 mm/s or 11%. Reduction of thermal conductivity by 20% results in decrease of reaction front movement from 0.36 mm/s to 0.33 mm/s or 8%. Reduction of thermal conductivity brings the reaction front movement closer to experimental measurement. The uncertainty of the correct thermal conductivities may be the main reason the model predicts faster reaction front movement than measured in experiments.

To study the impact of surface heat loss on the reaction system, the emissivity of the pellet was varied because the emissivity of the product is not clearly established. Radiative heat loss is dominant – one order of magnitude higher than convection heat loss – and affects the temperature more severely. The emissivity was increased to 0.7 and 0.9.

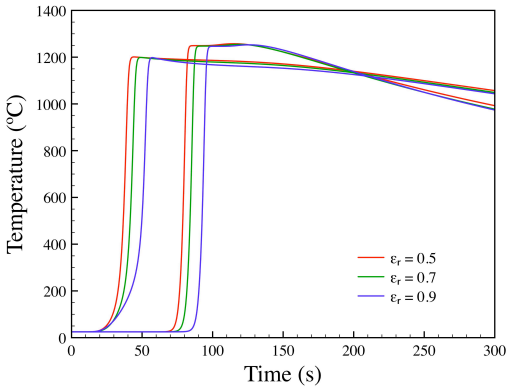

Figure 5. Effect of radiative heat loss on the temperature in the center of the pellet.

From Figure 5, it can be seen that increasing surface heat loss will slow down the reaction initially. The temperature at x = 1.0 cm reaches its maxima faster if lower surface emissivities are used but the reactivation front speed (distance between two points) remains the same. Also, the temperature at the centerline of the pellet is unaffected by the surface heat loss increase.

Surface temperature and cooling rate is affected by the increased radiative heat loss. Although the maximum temperature remains unchanged, rate of cooling on the surface is increased, resulting in a lower temperature after 300 seconds after the ignition.

5. Conclusions

Two-dimensional model of SHS reaction was successfully developed with COMSOL Multiphysics. Temperature profile agreed well with experimental data, especially during heating up period. It was shown that increase in the surface heat loss has negligible effect on reaction temperature and reaction front propagation speed. The model suggests that the speed of reaction front is strongly dependent on thermal conductivity of the material. Generated model is very flexible and can be used to study SHS reactions of other systems by changing thermodynamic and physical properties.

6. Nomenclature

c	concentration of product (mol/m^3)
C_p	specific heat capacity (J/kg K)
E	activation energy (J/mol)
h_c	heat transfer coefficient (W/m^2 K)
k	thermal conductivity (W/m K)
k_r	pre-exponent (1/s)
n	reaction order
Q	heat source (W/m^3)
q_0	inward heat flux (W/m^2)
q_{ign}	ignition heat flux (W/m^2)
R	gas constant (J/ K mol)
R_c	reaction rate (mol/m^3 s)
T	temperature (K)
t	time (s)
u	velocity vector (m/s)
ΔH_r	enthalpy of reaction (J/mol)
ε	porosity
ε_r	emissivity
η_r	product conversion
ρ	density (kg/m^3)
σ	Stefan–Boltzmann constant (5.67x10^{-8}W/ m^2 K^4)

7. References

1. Lawrence Livermore National Laboratory, Energy Flow Charts, https://publicaffairs.llnl.gov/news/energy/energy.html (accessed September 2010).

2. Rowe, D. M. *CRC Handbook of Thermoelectrics;* CRC Press LLC: Boca Raton, FL, USA (1995)

3. Autoblog, 2009. BMW's continued Efficient Dynamics plan to include thermoelectric generators http://green.autoblog.com/2009/03/09/bmws-continued-efficient-dynamics-plan-to-include-thermoelectri/ (accessed September 2010).

4. Hejtmánek, J.; Veverka, M.; Knizek, K.; Fujishiro, H.; Hebert, S.; Klein, Y.; Maignan, A.; Bellouard, C.; Lenoir, B. Cobaltites as perspective thermoelectrics. *Mater. Res. Soc. Symp. Proc.*, **886**, 0886-F01-07.1-9 (2006)

5 Sugiyama, J. ToyotaCRDL Rept_sugiyama. *R&D Review of Toyota CRDL*, **39**, 50-62 (2004)

6. Snyder, G.; Toberer, E. Complex thermoelectric materials. *Nature Materials*, **7**, 105-114 (2008)

7. Lin, S; Selig, J; Self-propagating High-temperature Synthesis of $Ca_{1.24}Co_{1.62}O_{3.86}$ thermoelectric powders, *Journal of Alloys and Compounds*, **503**, 402-409 (2010)

8. Merzhanov, A. G.; Borovinskaya, I. P. Self-propagated high-temperature synthesis of

refractory inorganic compounds. *Doklady Akademii Nauk*, **204**, 366-369 (1972)
9. Dandekar, H. W.; Puszynski, J. A.; Hlavacek, V. Two-dimensional numerical study of cross-flow filtration combustion. *AIChE Journal*, **36**, 1649-1660 (1990)
10. Varma, A.; Cao, G.; Morbidelli, M. Self-propagating solid-solid noncatalytic reactions in finite pellets. *AIChE Journal*, **36**, 1032-1038 (1990)
11. Holman, J. P.; Heat Transfer 9th ed., McGraw Hill, New York, NY (2002)